ARCTIC
VOL. 54, NO. 2 (JUNE 2001) P. 142–148

Climate Change Scenarios for Hudson Bay, Canada, from General Circulation Models

WILLIAM A. GOUGH[1,2] and EDMUND WOLFE[1]

(*Received 16 May 2000; accepted in revised form 19 September 2000*)

ABSTRACT. Two generations of a climate model are compared using the impact of a CO_2 doubling on the Hudson Bay region as the means of diagnosing differences in model performance. Surface temperature, precipitation, sea-ice coverage, and permafrost distribution are compared. The most striking difference is the response of the sea ice in the two models. In the coupled atmosphere-ocean climate model, sea ice virtually disappears in Hudson Bay. This leads to a substantially higher regional temperature response. We suggest that conductivity of sea ice and thermal diffusivity of seawater are key factors that cause the difference in sea-ice response. It is recommended that a regional model be developed to produce more representative climate change scenarios for the Hudson Bay region.

Key words: Hudson Bay, climate modeling, climate change scenarios, sea ice, permafrost, global warming

RÉSUMÉ. On compare deux générations d'un modèle de climat en calculant l'incidence sur la région de la baie d'Hudson d'une multiplication par deux du taux de CO_2 afin de diagnostiquer les différences dans la performance des deux versions du modèle. On compare la température en surface, les précipitations, la couverture de glace de mer et la distribution du pergélisol. La différence la plus marquante apparaît dans la façon dont la glace de mer réagit dans les deux modèles. Dans le modèle de climat avec couplage atmosphère-océan, la glace de mer disparaît pratiquement de la baie d'Hudson. Il en résulte une hausse notable de la température régionale. On suggère que la conductivité de la glace de mer et la diffusivité thermique de l'eau de mer sont des facteurs clés responsables de la différence dans le comportement de la glace de mer. On recommande l'élaboration d'un modèle régional qui créerait des scénarios de changement climatique plus réalistes pour la région de la baie d'Hudson.

Mots clés: baie d'Hudson, modélisation climatique, scénarios de changement climatique, glace de mer, pergélisol, réchauffement planétaire

Traduit pour la revue *Arctic* par Nésida Loyer.

INTRODUCTION

One of the most striking features of the Hudson Bay region is the complete annual cryogenic cycle. August and September are generally completely ice free, but sea ice begins to form in November and persists typically until June. The presence of this vast ice blanket has a tremendous impact on the regional climate. Rouse (1991) describes this influence as the 'winterization' of summer. Persistent sea ice delays the onset of spring and allows for the southern extension of permafrost along the western and southwestern coasts of Hudson Bay. The moderating effect of the Bay waters during the winter is literally cut off by the complete ice cover. The ice acts as an insulator, blocking the heat release from the Bay, mitigating land/sea differences during winter.

These unusual conditions have led to a unique ecosystem involving a vast range of species. This system is symbolized by the polar bear, the top of the food chain. Polar bears use the ice as a platform to hunt seals during the winter and spring. The bears increase in weight sufficiently to survive the summer and fall months on land, where food is scarce. Thus the continued presence of sea ice is essential for the survival of the polar bear in this region, and climate change poses a potential threat to the bear population (Stirling and Derocher, 1993; Stirling et al., 1999).

The presence of sea ice–induced permafrost has a substantial impact on the communities along the western coast of Hudson Bay (Wolfe, 1999). For example, coastal communities and transportation networks are now specially designed to prevent permafrost degradation in the built environment. Climate warming is likely to cause a significant shift in the distribution of permafrost (Woo et al., 1992) and thus in the built environment of the western coastal communities of Hudson Bay.

To assess the impact of climate change on the Hudson Bay region, climate change scenarios are needed. These can take the form of climate analogues, synthetic scenarios, or general circulation model (GCM) scenarios (Carter et al., 1996). In climate analogues, spatially or temporally displaced climate data are used as climate change scenarios. For example, this type of model has been used to assess water levels in the Great Lakes (Mortsch

[1] Environmental Science, University of Toronto at Scarborough, 1265 Military Trail, Scarborough, Ontario M1C 1A4, Canada
[2] Corresponding author: gough@scar.utoronto.ca

and Quinn, 1996). Synthetic scenarios use reasonable but idealized climate changes, such as 1˚C, 2˚C, or 3˚C warming. Gough (1998a) used a synthetic scenario of 3˚C to assess future sea levels in the Hudson Bay region. This scenario was loosely based on the results of general circulation models (Kattenberg et al., 1996). General circulation models are sophisticated, mathematically based simulations of the world's climate including atmospheric, oceanic, cryospheric, and land surface components.

Two types of warming scenarios have been developed. Older simulations examined the difference between two equilibrium simulations, one with the present CO_2 levels ($1 \times CO_2$) and a second with twice the current levels of CO_2 ($2 \times CO_2$). More recent simulations have examined the transient response to gradually increasing CO_2 levels. Typically a CO_2 doubling is linearly increased over a period of 70 to 100 years. The large thermal inertia of the ocean component of the model prevents an assessment of a new climate equilibrium. The transient response of the ocean to gradual changes in the atmosphere is substantially different from the equilibrium response (Gough and Lin, 1992). Most climate change impact assessments, however, have used the first type of scenario (e.g., Woo et al., 1992; Cohen et al., 1994). Thus it is of interest to compare the two types of GCM scenarios.

We examine here the two types of warming scenarios from two versions of the Canadian generation circulation model (Boer et al., 1992; McFarlane et al., 1992; Boer et al., 2000; Flato et al., 2000), focusing on the sensitive Hudson Bay region.

METHODS AND ANALYSIS

Models

Our analysis uses the results from two models. The first is the second generation of the Canadian general circulation model (GCM II). The atmospheric component is a sophisticated atmospheric general circulation model. The ocean component is represented as a simple two-layer slab ocean 50 m thick. Horizontal redistribution of ocean heat is prescribed in order to reproduce climatological values of sea surface temperatures and sea-ice distributions. Once a grid point is ice-covered, a prescribed under-ice heat flux replaces the slab ocean. The heat flux is prescribed so as to produce current sea-ice distribution as described in McFarlane et al. (1992). They also used a simple thermodynamic ice model that consists of both an ice layer and a snow layer and represents leads as fractional ice coverage. For further details, see Boer et al. (1992). Two simulations were used. In the first, CO_2 levels were fixed at current levels. In the second, CO_2 levels were doubled. Both simulations were run to equilibrium. Twenty years of simulation data were available for analysis. These simulations have been cited in the climate change assessments of Woo et al. (1992) and Cohen et al. (1994).

The second model is the Canadian first-generation coupled general circulation model (CGCM I). This model results from the coupling of the model described above (GCM II) with an ocean general circulation model replacing the slab ocean. Hudson Bay is represented by several dynamic vertical levels. Flux corrections are employed in order to reproduce current climatology. Two 200-year simulations beginning in 1900 are used: a control simulation using current greenhouse gas levels and a greenhouse gas increase scenario. After 1995, greenhouse gases were increased at the rate of 1% per year with a corresponding increase in sulphate aerosols (Boer et al., 2000; Flato et al., 2000). This increase simulation will be referred to subsequently as GHGA. Flato et al. (2000) reported on the ability of the model to reproduce broad features of the current climate successfully; however, they noted lower fidelity at the regional scale.

Since both models have the same spatial resolution, both represent Hudson Bay as a group of eleven grid points forming an enclosed sea. In the coupled model, there is a diffusive link to the rest of the ocean via Hudson Strait, although it is not a dynamic link like that found in some other world ocean representations (Gough and Allakhverdova, 1999).

The coarse resolution of the climate model and the simplification of model components required to run the models efficiently necessitate caution in the use of such model output. Gough and Allakhverdova (1999) examined the coarse grid representation of Hudson Bay and surrounding waters using a similar ocean general circulation model, in which Hudson Bay formed an advective link with the Labrador Sea by suppressing the orography of Baffin Island. However, they concluded that the advective link played a relatively minor role in determining the response of Hudson Bay sea ice to climate change scenarios. Far more important was the sensitivity to model parameters such as the thermal conductivity of sea ice and the thermal diffusivity of seawater as shown in a follow-up study (Gough, in press). Thermal diffusivity is a parameter that accounts for sub–grid scale processes such as mesoscale eddies, internal wave breaking, double diffusion, and small-scale convection. Gough and Allakhverdova (1998) have also shown that modest variations of vertical and horizontal diffusivity in an ocean general circulation model have more impact on ocean flow and tracer uptake than did typical warming scenarios.

Analysis

For the Hudson Bay region, we used data from 53.81 to 68.65˚N and from 97.5 to 71.25˚W. This area consisted of 40 grid points, of which 12 were ocean points (11 for Hudson Bay and Foxe Basin and 1 for Hudson Strait) and 28 were surrounding land points. Surface temperature, precipitation, sea-ice cover, and number of permafrost points were examined. To illustrate the influence of ice cover, land and ocean points were analyzed separately. For

TABLE 1. Annual average surface temperatures (°C) for GCM II and CGCM I simulations.

Simulation	1 x CO_2 (land)	1 x CO_2 (ocean)	2 x CO_2 (land)	2 x CO_2 (ocean)	2 x CO_2 - 1 x CO_2 (land)	2 x CO_2 - 1 x CO_2 (ocean)
GCM II	-7.5	-6.2	-2.4	-1.6	5.1	4.6
CGCM I	-6.7	-4.9	-2.4	1.6	4.4	6.5
CGCM I-GCM II	0.8	1.3	0.0	3.2	-0.7	1.9

TABLE 2. Annual average precipitation (mm/month) for GCM II and CGCM I simulations.

Simulation	1 x CO_2 (land)	1 x CO_2 (ocean)	2 x CO_2 (land)	2 x CO_2 (ocean)	2 x CO_2 - 1 x CO_2 (land)	2 x CO_2 - 1 x CO_2 (ocean)
GCM II	24.0	20.6	27.2	24.7	3.2	4.1
CGCM I	24.5	21.4	26.3	22.2	1.8	0.8
CGCM I-GCM II	0.5	0.8	-0.9	-2.5	-1.4	-3.3

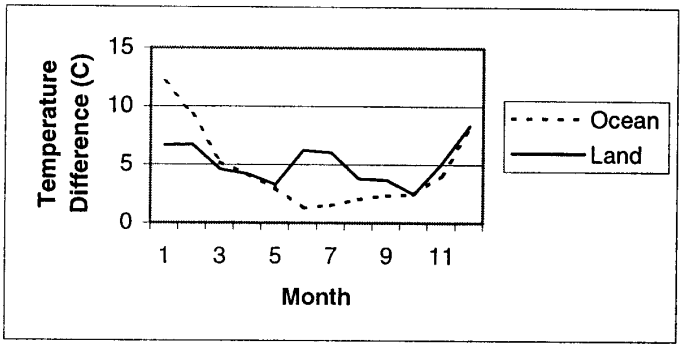

FIG. 1. Temperature difference (°C) for GCM II, 2 × CO_2 - 1 × CO_2.

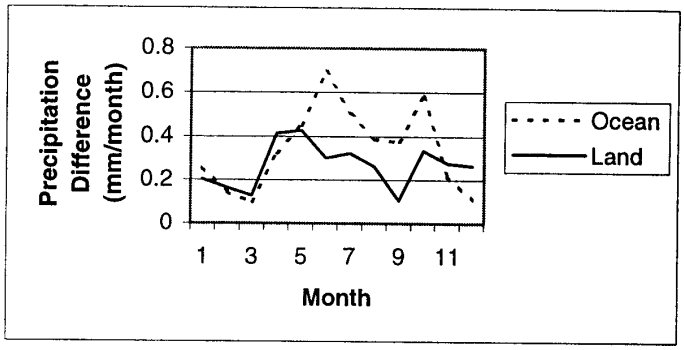

FIG. 2. Precipitation difference (mm/month) for GCM II, 2 × CO_2 - 1 × CO_2.

the GCM II results, ice cover was deduced from surface temperature. For the CGCM I results, sea-ice data were directly available.

The GCM II data consisted of two 19-year equilibrium simulations, one for 1 × CO_2 and the other for 2 × CO_2. The CGCM I data analyzed consisted of two 200-year simulations (from 1900 to 2100). For purposes of comparison to the GCM II results, the CGCM I control simulation is considered to be the 1 × CO_2 case, and the CGCM I GHGA simulation is considered to be the 2 × CO_2 case, using a 10-year average centred at 2050. Because of the thermal lag of the world ocean, it is likely that the full effect of the CO_2 doubling has not yet been felt, even though the concentration has doubled (relative to the 1980s) by this time. Thus, these results may represent a slight underestimate of 2 × CO_2.

RESULTS

GCM II

On average, the Hudson Bay regional temperatures increase by 5.0°C. This increase, which combines a 5.1°C rise in land temperatures and a 4.6°C rise in ocean temperatures (Table 1) for 2 × CO_2, compares to a 3.5°C warming globally (Boer et al., 1992). Figure 1 depicts the annual cycle of temperature differences between 2 × CO_2 and 1 × CO_2 for land and ocean. The warming for both land and ocean is amplified in the winter, with the greatest warming occurring in January over the ocean. The land warming experiences a secondary peak in June and July. The ocean peak is likely the result of sea-ice depletion, as will be seen below. The summer land peak is likely due to a drier land surface: greater evaporation leads to drier soil under warming conditions.

When CO_2 is doubled, precipitation increases by 15% in the Hudson Bay region (Table 2) compared to a 4% increase globally. The increase tends to be larger (20%) over the ocean. Figure 2 shows the annual cycle of precipitation differences for ocean and land. The greatest increase in precipitation occurs in the spring and summer months, May, June, and July, corresponding to earlier ice breakup. A secondary peak in October corresponds to later freeze-up. The seasonal bias of the precipitation change is particularly notable for the ocean.

Ice distribution is determined by examining the temperature of the ocean points. Complete ice cover occurs when all twelve ocean points are below -2.0°C. Annually, 6.3 points are ice-covered on average for the 1 × CO_2 climate, and 4.6 points for the 2 × CO_2 climate (Table 3). Figure 3 shows the average distribution of ice by plotting the number of grid points covered by ice ("sea ice points") as a function of the month of the year. For the 1 × CO_2 simulation, all points are completely ice covered for four months (January through April) and completely ice free

TABLE 3. Annual average number of sea-ice points for GCM II and CGCM I. Total number of ocean points is twelve.

Simulation	1 x CO_2	2 x CO_2	2 x CO_2 - 1 x CO_2
GCM II	6.3	4.6	-1.7
CGCM I	7.8	2.5	-5.4
CGCM I-GCM II	1.5	-2.1	-3.7

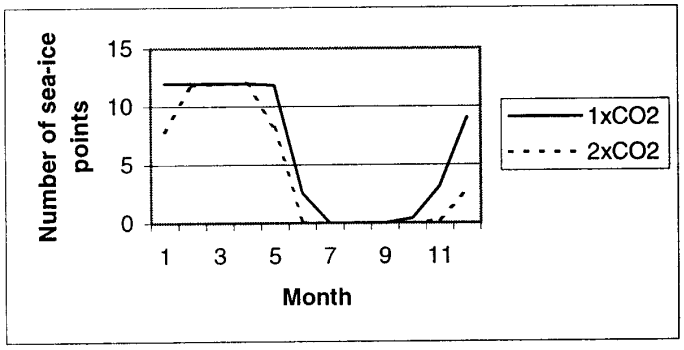

FIG. 3. Average annual cycle of sea-ice coverage for GCM II, expressed as number of ice-covered grid points. Twelve grid points represent complete sea-ice coverage.

TABLE 4. Annual average number of permafrost points. For the Hudson Bay region, a permafrost point is defined as a grid point for which the annual average temperature is colder than -5.0°C.

Simulation	1 x CO_2	2 x CO_2	2 x CO_2 - 1 x CO_2
GCM II	18.3	10.6	-7.7
CGCM I	17.9	9.2	-8.7
CGCM I-GCM II	-0.4	-1.4	-1.0

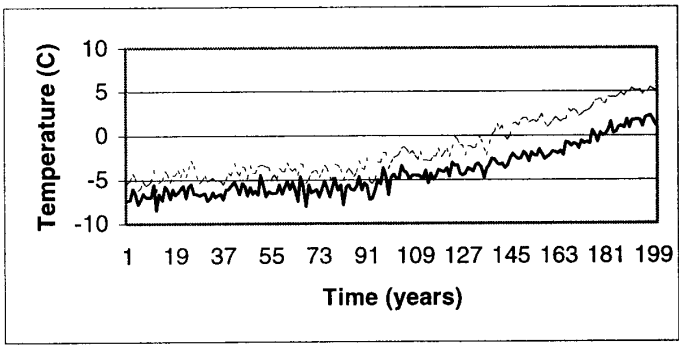

FIG. 4. Temporal evolution of surface temperature (˚C) for CGCM I. The solid line represents land temperatures. The dashed line represents ocean temperatures.

for three months. This result is in reasonable agreement with observations (Gough and Allakhverdova, 1999). For the CO_2 doubling case, all points are completely ice covered for three months and ice-free for five months. Spring breakup takes place approximately one month earlier and freeze-up begins a month later than in the 1 × CO_2 case. The earlier breakup coincides with the timing of increased spring precipitation. Once the ice cover melts, the region gains a large source of potential water vapour. The later freeze-up coincides with the largest temperature difference over ocean points in January. With incomplete ice cover, the Bay waters act as a local heating source.

The line of continuous permafrost in the Hudson Bay region occurs around the -5˚C annual isotherm (Cohen et al., 1994). The temperature data were re-examined using this threshold to determine how many of the 28 land points met this criterion. In the 1 × CO_2 simulation, 18.3 points on average satisfied the permafrost criterion (Table 4), with a standard deviation of 1.0 for the 19-year simulation. For the 2 × CO_2 simulation, 10.6 points on average qualified as permafrost, with a standard deviation of 1.8. This represents a reduction of approximately 42%. The average land point temperature increased from -7.5˚C to -2.4˚C (Table 1).

CGCM I

As discussed above, the methodology for the coupled model (CGCM I) simulations was different from that used for GCM II. Rather than a 2 × CO_2 equilibrium simulation, a series of 200-year simulations beginning at 1900 were done. For this analysis, we focus on the temporal evolution of the simulation, emphasizing the difference between periods in the time series. In addition, we compare two of the 200-year simulations, one with no future increases in CO_2 and aerosols (control) and the other with 1% per year increases in CO_2 and equivalent increases in aerosols (GHGA). In the results below, these two simulations are compared to the GCM II 1 × CO_2 and 2 × CO_2 scenarios, respectively.

Table 1 lists the annual averages for land and ocean temperatures. The CGCM I results are approximately 1˚C warmer than the GCM II results for the 1 × CO_2 (control) simulations. In addition, for CO_2 doubling, the ocean is almost 2˚C warmer and land is 0.7˚C cooler in the CGCM I than in the GCM II results. Figure 4 depicts the evolution of land and ocean temperatures over 200 years for the coupled simulation (GHGA). The ocean temperature increases by 6.5˚C and the land temperature by 4.4˚C compared to the control run. Figure 5 shows a time series of the difference between the average temperatures on land and ocean. For the early years of the simulation, up to approximately year 2035, the difference between land and ocean temperatures hovers around 2˚C. After 2035, the temperature difference jumps to over 3.5˚C. This jump corresponds to an increase in the number of ice-free points, as shown below. Complete ice cover enables the ocean temperature to fall well below the freezing point because of the insulating properties of the sea ice. Once this ice cover is no longer present, the intense winter cooling of the ocean is limited to about -2˚C, the freezing point of seawater.

The CGCM I precipitation was marginally (2–4%) higher than in the GCM II results for the 1 × CO_2 simulations. However, precipitation increased by only 5% for the 2 × CO_2 simulation, considerably less than in the GCM II simulation. There is an asymmetric response for land and ocean. In the GCM II simulation, the ocean precipitation increases more than the precipitation on land, while the opposite is true for the CGCM I simulations. The reason for this result is unclear.

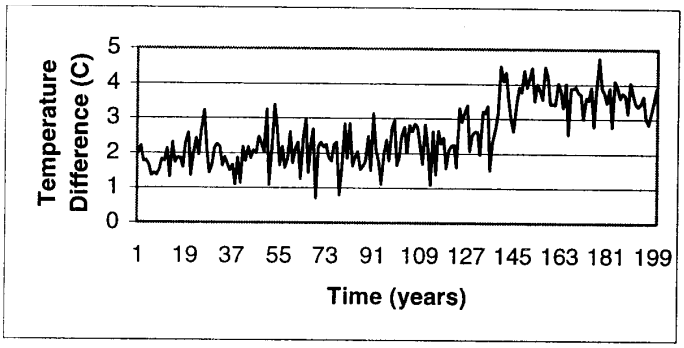

FIG. 5. Temporal evolution of temperature difference (°C) between ocean and land points for CGCM I.

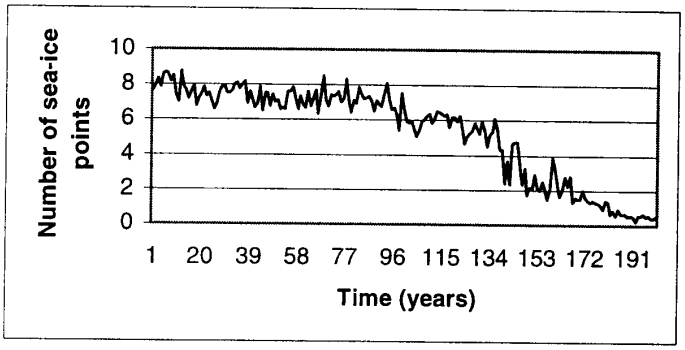

FIG. 6. Sea-ice point count for 200-year CGCM I simulation. Greenhouse gases increase at a rate of 1% per year after 1995, with corresponding changes to aerosols.

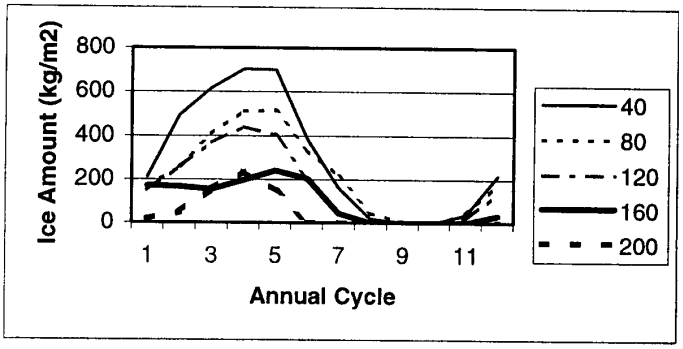

FIG. 7. Sea ice amount (kg/m^2): seasonal cycle at 40-year intervals for CGCM I.

The average number of sea-ice points (7.8, see Table 3) for the CGCM I simulation is higher than in the GCM II simulation (6.3) for the $1 \times CO_2$ simulations. The response to a CO_2 doubling, however, is more dramatic, so that the annual average number of sea-ice points is lower for the CGCM I simulation (2.5, versus 4.6 for GCM II). Figure 6 shows the annual average as a function of time. In the 20th century, the value hovers around 7.0, dropping to 6.0 shortly after the imposition of the 1% per year increase. Around 2035 there is a further decrease to 2.0 points on average, and this figure falls below 1.0 by the end of the simulation. To illustrate the seasonal impact of this evolution, Figure 7 depicts the ice amount in kg/m^2 at five different times (in 1940, 1980, 2020, 2060, and 2100). By 2100, the only remaining ice occurs at the two most northern points (Foxe Basin) and persists only for a few months. A comparison of the curves for 2020 and 2060 shows a dramatic change in sea-ice amount. This change corresponds to the drop in the number of sea-ice points around 2035 and the increase in average ocean temperature.

The number of permafrost points shows the least difference between models of all the diagnostics examined. The CGCM I simulations have a marginally smaller number of permafrost points (17.9, see Table 4). The reduction of permafrost points was slightly higher for the GHGA scenario even though the warming over land was less for CGCM I than for the corresponding GCM II points. This seeming contradiction arises because the CGCM I land temperatures for $1 \times CO_2$ are closer to the -5°C permafrost threshold and thus are more sensitive to temperature change. The close agreement between models is likely the result of all permafrost points being on land, since the ocean points displayed a greater and more variable response to CO_2 doubling. In a spatial analysis of permafrost points for both models (not shown), permafrost exists on the eastern and western coasts of Hudson Bay. However the distribution is symmetric, contrary to observations, and there are no permafrost points on the southern shore of Hudson Bay, which is also inconsistent with observations. These inconsistencies suggest that neither model captures the Bay's modifying effect, which produces frost points well south of those in surrounding regions.

DISCUSSION

Climate change impact assessments rely on climate change scenarios, which are commonly obtained from sophisticated climate models (Carter et al., 1996). In this work, we have examined the results from two generations of the Canadian climate model for the Hudson Bay region.

The more recent results (CGCM I) have a muted thermal response to a $2 \times CO_2$ scenario for land but a more dramatic change in sea ice. Sea-ice coverage virtually disappears. This has important consequences for the regional climate and local biota, such as the local polar bear populations (Stirling et al., 1999). Under the GCM II results, the ice platform remains; however, it disappears for the most part in the CGCM I results.

Since the stakes are so high, it is important to assess the cause of the difference and the issues related to our dependence on modelling. Gough and Allakhverdova (1999) and Gough (in press) have examined the importance of the representation of ocean bathymetry and the model parameterization of sea-ice conductivity and seawater diffusivity. Gough and Allakhverdova (1999) concluded that model parameterization played a more important role than ensuring an advective link into Hudson Bay from the Labrador Sea. Gough (in press) showed that numerous different combinations of the vertical diffusivity of seawater and thermal conductivity of sea ice can correctly reproduce current sea-ice climatology (as measured by the peak

sea-ice thickness). For larger values of thermal conductivity, the thermal diffusivity needed to be increased to achieve the same ice thickness. However, it was also found that these different combinations produced very different responses to a climate warming. The thermal diffusivity was the dominant factor in determining the response to a climate warming: the larger the value of the thermal diffusivity, the larger the response in ice-thickness changes. A similar thermodynamic ice model was used in both the GCM II and the CGCM I simulations, but the representation of the oceans differed. The CGCM I model had an ocean model with a vertical diffusivity of 0.3 cm^2/s, at the low end of values typically used in ocean modelling (Gough, 1998b). It also had a diffusive link through Hudson Strait and used flux corrections. In the GCM II, the 50 m slab ocean was replaced after ice formation by under-ice heat fluxes. These fluxes were adjusted to reproduce current sea-ice climatology. As a tuning exercise, this is equivalent to tuning to the vertical diffusivity, as was done in Gough (in press). The differences between GCM II and CGCM I results suggest that the under-ice heat flux tuning for the GCM II is equivalent to a vertical diffusivity lower than that used in the CGCM I. That is, there is greater ice reduction in the CGCM I simulation for a CO_2 doubling. This strong dependence on model parameterization suggests that climate change scenarios derived from general circulation models must be used with caution.

The comparison of the various simulations of the impact of CO_2 doubling on Hudson Bay revealed substantially different responses in sea-ice distribution. This is a key issue for the Bay region because the ice distribution has a dominating influence on the local climate and biota. To resolve this issue, we recommend developing a regional model that can be embedded into a larger scale model (such as that of the Canadian Centre for Climate Modelling and Analysis [CCCma]). This type of modelling allows for the finer resolution needed in the Hudson Bay region but without the exorbitant computational overhead of a uniformly fine grid model (Giorgi, 1990; McGregor, 1997). Regional model capability has been developed for the CCCma model (Caya et al., 1995; Laprise et al., 1998; Caya and Laprise, 1999). Development of a regional model based on the CCCma model would allow a more accurate representation of the bathymetry of Hudson Bay, the interaction with the Labrador Sea and Foxe Basin, and the parameters of sea-ice conductivity and thermal diffusivity of seawater.

ACKNOWLEDGEMENTS

We wish to thank Drs. F. Zwiers and G. Flato of the Canadian Centre for Climate Modelling and Analysis for providing the model output. We acknowledge the helpful comments of several reviewers.

REFERENCES

BOER, G.J., McFARLANE, N.A., and LAZARE, M. 1992. Greenhouse gas–induced climate change simulated with the CCC second-generation general circulation model. Journal of Climate 5:1045–1077.

BOER, G.J., FLATO, G., and RAMSDEN, D. 2000. A transient climate change simulation with greenhouse gas and aerosol forcing: Projected climate to the twenty-first century. Climate Dynamics 16:427–450.

CARTER, T., PARRY, M., NISHIOKA, S., and HARASAWA, H. 1996. Technical guidelines for assessing climate change impacts and adaptations. In: Watson, R.T., Zinyowera, M.C., and Moss, R.H., eds. Climate change 1995. Impacts, adaptations and mitigations of climate change: Scientific-Technical Analyses. Cambridge: Cambridge University Press. 823–834.

CAYA, D., and LAPRISE, R. 1999. A semi-implicit semi-Lagrangian regional climate model: The Canadian RCM. Monthly Weather Review 127:341–362.

CAYA, D., LAPRISE, R., GIGUERE, M., BERGERON, G., BLANCHET, J.-P., STOCKS, B.J., BOER, G.J., and McFARLANE, N.A. 1995. Description of the Canadian regional climate model. Water, Air, and Soil Pollution 82:477–482.

COHEN, S., AGNEW, T., HEADLEY, A., LOUIE, P., REYCROFT, J., and SKINNER, W. 1994. Climate variability, climatic change, and implications for the future of the Hudson Bay bioregion: The Hudson Bay Project 1994. Ottawa: Environment Canada. 112 p.

FLATO, G., BOER, G.J., LEE, W.G., McFARLANE, N.A., RAMSDEN, D., READER, M.C., and WEAVER, A.J. 2000. The Canadian Centre for Climate Modelling and Analysis global model and its climate. Climate Dynamics 16:451–467.

GIORGI, F. 1990. Simulations of regional climate using a limited area model nested in a general circulation model. Journal of Climate 3:941–963.

GOUGH, W.A. 1998a. Projections of sea-level change in Hudson and James Bays, Canada due to global warming. Arctic and Alpine Research 30:84–88.

———. 1998b. Estimating sub–grid scale processes using oceanographic data. Elements of Change 1997. Proceedings of Aspen Global Change Institute Workshop on Upscaling of Site Specific Measurements. Aspen, Colorado: Aspen Global Change Institute. 52–56.

———. In press. Model tuning and impacts on climate change assessment: Hudson Bay, a case study. The Canadian Geographer 45.

GOUGH, W.A., and ALLAKHVERDOVA, T. 1998. Sensitivity of a coarse resolution ocean general circulation model under climate change forcing. Tellus 50A:124–133.

———. 1999. Limitations of using a coarse resolution model to assess the impact of climate change on sea ice in Hudson Bay. The Canadian Geographer 43:415–422.

GOUGH, W.A., and LIN, C.A. 1992. The response of an ocean general circulation model to long time-scale surface temperature anomalies. Atmosphere-Ocean 30:653–674.

KATTENBERG, A., GIORGI, F., GRASSL, H., MEEHL, G.A., MITCHELL, J.F.B., STOUFFER, R., TOKIOKA, T., WEAVER, A.J., and WIGLEY, T.M.L. 1996. Climate models - Projections

of future climate In: Houghton, J.T., Meira Filho, L.G., Callander, B.A., Harris, N., Kattenberg, A., and Maskell, K., eds. Climate change 1995: The science of climate change. Cambridge: Cambridge University Press. 285–358.

LAPRISE, R., CAYA, D., GIGUERE, M., BERGERON, G., BOER, G.J., and McFARLANE, N.A. 1998. Climate and climate change in western Canada as simulated by the Canadian regional climate model. Atmosphere-Ocean 36:119–167.

McFARLANE, N.A., BOER, G.J., BLANCHET, J.-P., and LAZARE, M. 1992. The Canadian Climate Centre second-generation general circulation model and its equilibrium climate. Journal of Climate 5:1013–1044.

McGREGOR, J.L. 1997. Regional climate modelling. Meteorology and Atmospheric Physics 13:105–117.

MORTSCH, L., and QUINN, F.H. 1996. Climate change scenarios for Great Lake Basin ecosystem studies. Limnology and Oceanography 41:903–911.

ROUSE, W.R. 1991. Impacts of Hudson Bay on the terrestrial climate of the Hudson Bay lowlands. Arctic and Alpine Research 23:24–30.

STIRLING, I., and DEROCHER, A.E. 1993. Possible impacts of climatic warming on polar bears. Arctic 46:240–245.

STIRLING, I., LUNN, N.J., and IACOZZA, J. 1999. Long-term trends in the population ecology of polar bears in western Hudson Bay in relation to climatic change. Arctic 52:294–306.

WOLFE, E. 1999. Permafrost: Human adaptation to climate change in the Hudson Bay region. M.A. thesis, University of Toronto, Toronto, Ontario, Canada. 105 p.

WOO, M., LEWKOWICZ, A.G., and ROUSE, W.R. 1992. Response of the Canadian permafrost environment to climatic change. Physical Geography 13:287–317.